Comparison of the structure and thermal properties of a poly(aryl ether ketone ether ketone naphthyl ketone) with those of poly(aryl ether ketone ether ketone ketone)

Marcel Dosière,[1] Didier Villers,[1] Mikhail G. Zolotukhin,[2] Michel H.J. Koch[3]*

[1] Laboratoire de Physicochimie des Polymères, Université de Mons - Hainaut, 20 Place du Parc, B-7000 Mons, Belgium; email : marcel.dosiere@umh.ac.be; didier.villers@umh.ac.be

[2] Instituto de Investigaciones en Materiales, Universidad Nacional Autonoma de Mexico, Apartado Postal 70-360, CU, Coyoacan, 04510, Mexico D.F, Mexico; email: zolotukhin@iim.unam.mx

[3*]European Molecular Biology Laboratory, Hamburg Outstation, EMBL c/o DESY, Notkestrasse 85, D-22603 Hamburg, Germany; email: koch@embl-hamburg.de

Abstract: Poly(oxy-1,4-phenylene carbonyl-1,4-phenylene oxy-1,4-phenylene carbonyl-2,6-naphthalene carbonyl-1,4-phenylene) or 2,6-PEKEKNK is a polymer of the poly(aryl ether ketone) family differing from PEKEKK by the presence of a naphthyl group linked at positions 2 and 6 to the two ketone groups. It is synthesized by electrophilic precipitation polycondensation of 2,6-naphthalenedicarboxylic acid chloride with 4,4'-bis-(4-phenoxy) benzophenone in the presence of aluminium chloride. The dimensions of the orthorhombic unit cell determined from an initially amorphous, stretched film are: a = 0.778 nm, b = 0.613 nm, c = 5.52 nm. In contrast with PEKEKK no signs of polymorphism were found for 2,6 PEKEKNK. Its glass transition and melting temperatures are 20 ºC and 2 ºC above those of PEKEKK, respectively.

Introduction

Poly(aryl ether ketone)s or PAEKs are a family of semicrystalline, high temperature, high performance engineering thermoplastics displaying a useful combination of physical, thermal and mechanical properties [1-3]. The commercial PAEKs (PEK, PEKK, PEEK, PEKEKK) only differ from each other by their ether/ketone (E/K) ratio in the chain. PEEK and PEK have orthorhombic unit cells similar to that of poly(phenylene oxide) (PPO) [4, 5], which can be considered as the limiting member of the family with 100% ether groups. It has been shown that as ether and ketone linkages can be interchanged with minimal distortions, the chain conformation of PPO could be used to describe two consecutive aryl units in PAEKs [6-8].

Structures differing from that of PPO were obtained for various PAEKs synthesized with specific spacers or with isomers of the reagents. Amongst others, the effect of diketone linkages [9], biphenyl and meta-phenyl units [10] and different para/meta phenyl isomer ratios [11] have been investigated.

PAEKs suffer from poor creep behavior due to their relatively low glass transition temperature compared to their melting temperature. In an effort to prepare polymers

with higher glass transition temperatures, new polyketones with naphthalenic groups in the main chain were prepared using precipitation polycondensation [12, 13]. The present paper describes the synthesis and some properties of one of these polymers, poly(oxy-1,4-phenylene carbonyl-1,4-phenylene oxy-1,4-phenylene carbonyl-2,6-naphthalene carbonyl-1,4-phenylene) in short 2,6-PEKEKNK. Incorporation of a bulky naphthyl group in the main chain increases the glass transition temperature significantly without much effect on the melting temperature. The crystal structure, polymorphism and cold crystallization of 2-6 PEKEKNK are compared to those of PEKEKK.

Results and discussion

The chemical composition of the polymers is shown below:
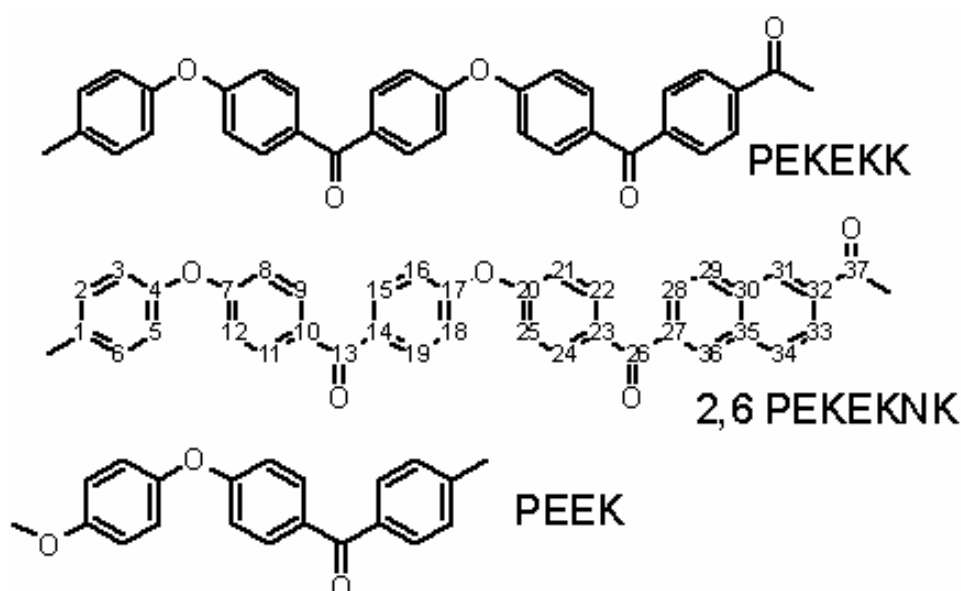
Synthesis and Molecular Characterization

2,6-PEKEKNK was synthesized by the Friedel-Crafts reaction of 2,6-naphthalenedicarboxylic acid chloride with 4,4'-bis-(4-phenoxy) benzophenone in the presence of aluminum chloride according to the scheme in Fig. 1.

The reaction is a typical electrophilic precipitation polycondensation [12, 13]. The transparent, colourless solution of diphenoxybenzophenone and 2,6-naphthalenedicarboxylic acid chloride in dichloroethane was cooled to -15 ^{0}C, aluminium chloride was added to the solution and the reaction mixture was stirred for 30 min. Thereafter, the temperature was raised to 20 ^{0}C over 2 h and the reaction was continued at this temperature for 20 h. In the course of synthesis, the reaction products precipitate as small particles after reaching a critical molecular mass. The suspension obtained was filtered, and pure polyketone particles were recovered by washing with methanol and extraction with boiling methanol for 20 h. After that, the particles were allowed to dry in air and were heated at 100 ^{0}C overnight under vacuum.

The polymer is soluble in strong acids (concentrated sulfuric acid, methane sulfonic acid or a trifluoroacetic acid-chloroform mixture).
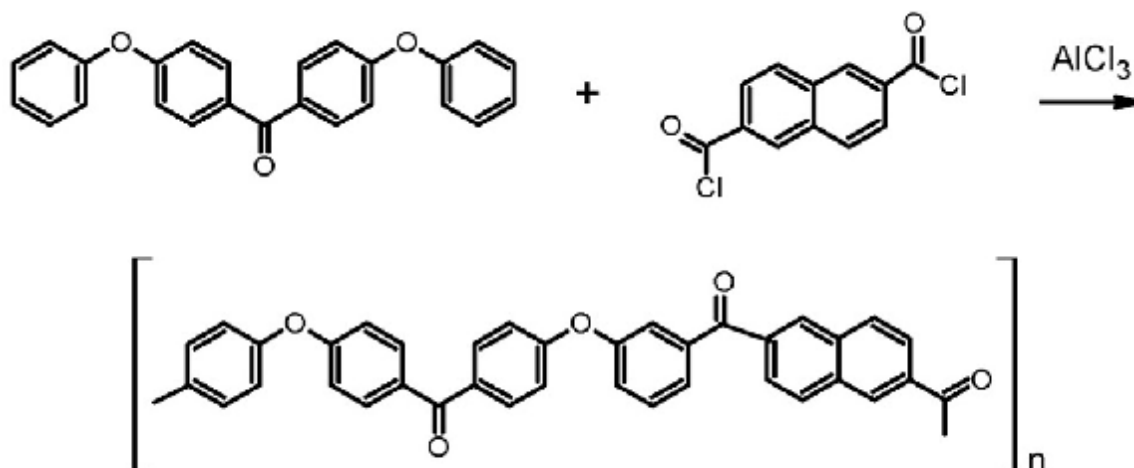

Fig. 1. Reaction scheme for the synthesis of 2,6-PEKEKNK.

Precipitation polycondensation relies on the fact that polymerization continues in precipitated particles yielding high molecular mass polymers and, as shown previously, the molecular mass is independent of the particles size [12]. As illustrated in Fig. 2, during preparation the intrinsic viscosity of the precipitated polymer increases over time, while that of the soluble polymer remains nearly constant.
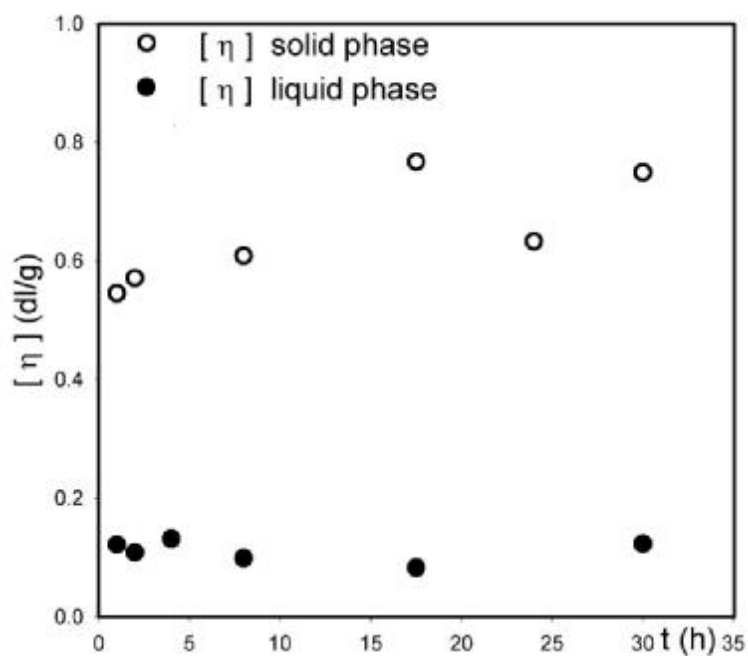

Fig. 2. Dependence of the intrinsic viscosity on the reaction time.

The intrinsic viscosity of the polymer precipitated during synthesis is approximately six times higher than that of the soluble one, as already observed in a similar synthesis [20]. The molecular mass of the polymer in the solid phase rapidly reaches a nearly constant value (~ 40,000) whereas the polymer obtained in solution has a molecular mass of only 8,000 (as determined using the Mark-Houwink-Sakurada relationship, with parameters adjusted for PEEK in CH_3SO_4 at 25 °C ([η] = $5.77.10^{-5}$ $Mw^{0.90}$ (dl/g)) [21]).

For morphological studies polymer particles obtained after additional washing and drying of the initial "as synthesized" powder were molten at 420 °C in a hydraulic press and quenched in cold water to obtain amorphous films of 2,6-PEKEKNK (density: 1.2692 $g.cm^{-3}$).

Oriented samples were obtained by drawing initially amorphous films to a ratio of 3 in an oven followed by annealing at 270 and 330 °C for several hours.

NMR

The selectivity of the Friedel-Crafts reaction was verified by establishing the structure of the polyketone by ^{1}H NMR spectroscopy, which seems more sensitive than ^{13}C NMR for aromatic polymers. ^{1}H NMR spectra were taken and analyzed as described previously [13, 20, 22]. The numbering of the carbon atoms and corresponding hydrogen atoms is shown in Figure 1.
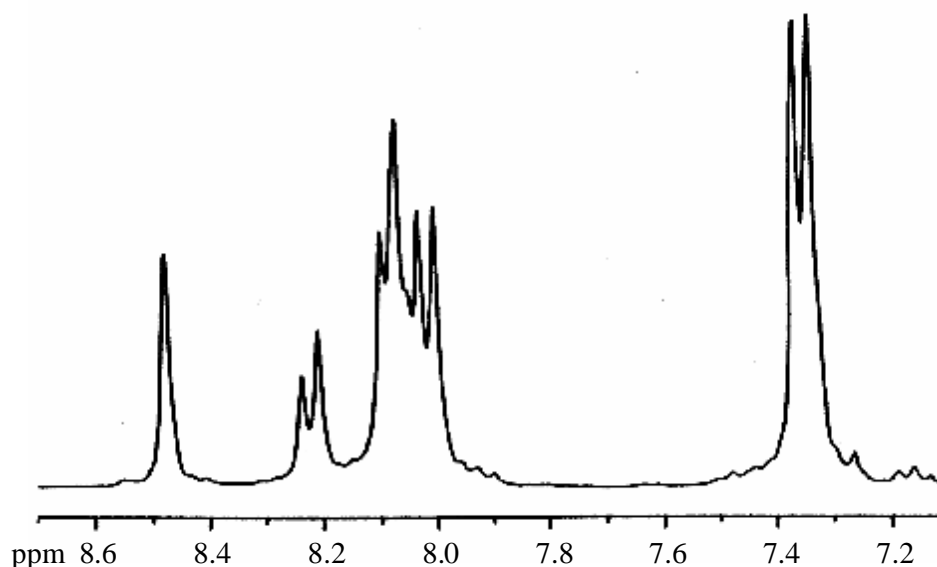

Fig. 3. ^{1}H NMR spectrum of 2,6-PEKEKNK.

The signals in the ^{1}H NMR spectrum in Figure 3 result from 22 H atoms in 5 different chemical environments in the repeating unit. The signals at 8.49 and 8.23 ppm are each associated with 2 protons and those at 8.05 and 7.35 ppm each with 8 protons and that at 8.11 ppm corresponds to the last two protons. The singlets at 8.49 correspond to H31 and H36, the doublet at 8.23 ppm to H28 and H33. The group near 8.1 ppm is due to H2, H6, H9, H11, H15, H22, H24, H29 and H34 and the doublet at 7.35 ppm to H3, H5, H8, H12, H16, H18, H21 and H25. The small signal

near 7.2 ppm results from impurities in CDCl$_3$ and the strong peak at 11.2 (not shown) to trifluoroacetic acid.

The absence of other signals due to e.g. organic impurities proves the purity of the 2,6-PEKEKNK sample. A small signal at 4 ppm (not shown) suggests that there is a very low level of meta or ortho branching on the phenyls during acylation. The assignment of the peaks at 8.49, 8.23 and 8.11 ppm to H31, H36, H28, H33, H29, H34 is based on the spectrum of naphthalene-2,6-dicarboxylic acid (not shown).

The 15 peaks in the ^{13}C NMR spectrum in Figure 4 are due to the 37 carbon atoms in the repeating unit. The triplet at 77.67 ppm corresponds to CDCl$_3$ and the two quadruplets at 162 and 115 ppm are associated with trifluoroactic acid. The carbonyl carbons give signals at 201.88 (C26 and C37) and 201.21 ppm (C13). Unambiguous identification of the other signals is more difficult but based on tabulated values for benzene ring signals, the following attributions were made: in the signals at 162.68 and 162.08 ppm to C4, C20, C7 and C17, the inverse configuration is equally likely. The signal at 137.53 ppm is associated with C27 and C32 and that at 135.68 ppm to C30 and C35. The signals at 134.99 and 134.64 ppm are respectively due to C9, C11, C15, C19 and C2, C6, C22 and C24 or the reverse. C31 and C36 give a signal at 133.35 ppm. The signals at 133.18 and 132.82 ppm can equally well be attributed to C1 and C23 as to C10, C14. The two signals at 131.45 and 127.8 ppm are associated with C28, C33 and C29, C34, whereas the signals at 120.33 and 120.14 ppm are due to C8, C12, C16, C18 and C3, C5, C21, C25. The absence of signals corresponding to ortho or meta branching in the main chain proves that the synthesis yields a linear homopolymer.
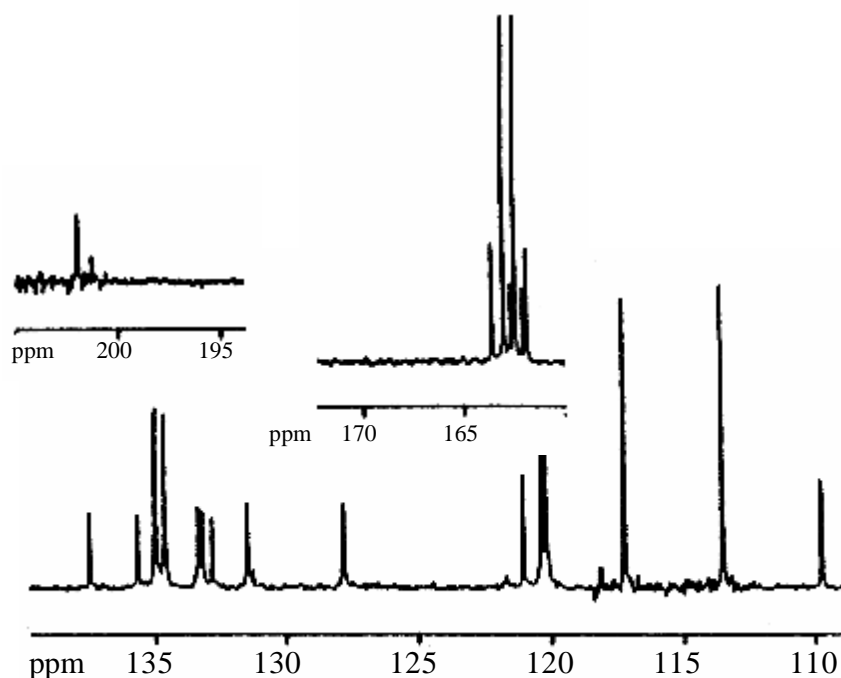

Fig. 4. ^{13}C NMR spectrum of 2,6-PEKEKNK.

DSC curves of amorphous samples of PEEK, PEKEKK and 2-6 PEKEKNK

The DSC heating curves of amorphous PEKEKK and 2,6-PEKEKNK and PEEK samples are shown in Fig. 5.

The corresponding thermal properties are summarized in Tab. 1. The glass transition of 2,6 PEKEKNK (T_g = 179 °C) is well above those of PEEK (146 °C) and PEKEKK (158 °C). The increase in specific heat are very similar for 2,6 PEKEKNK and PEKEKK ($\Delta C_p \cong$ 0.3 J/g K).

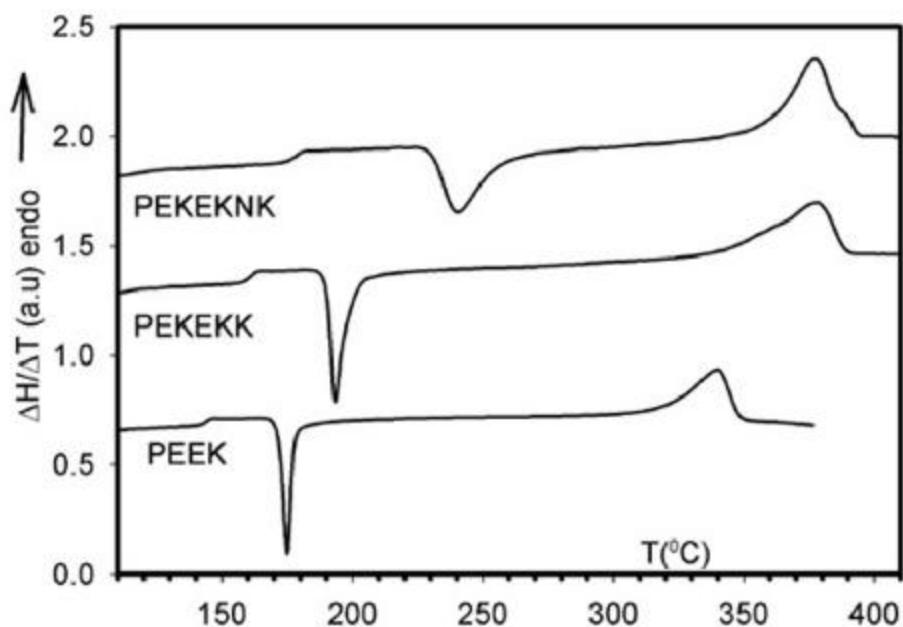**Fig. 5.** DSC heating curves recorded at 10 °C/min for amorphous PEEK, PEKEKK and PEKEKNK.

Tab. 1. Calorimetric data of PEKEKK and 2,6-PEKEKNK and PEEK.

PAEK	K/(E+K)	T_g/°C	ΔC_p(J/gK)	T_{cc}/°C	ΔH_c/(J/g)	ΔT_{cc}/°C	T_m/°C	ΔH_m(J/g)
PEKEKK	3/5	158	0.304	193	-31.4	5	378	42.0
PEKEKNK	3/5	179	0.312	242	-23.1	16	380	29.0
PEEK	1/3	146	0.20	175	-20.1	3	340	32.8

Glass transition temperature (T_g), specific heat step at the glass transition temperature (ΔC_p), cold crystallization temperature (T_{cc}) and heat (ΔH_{cc}) associated with the cold crystallization exotherm, melting temperature (T_m) and melting heat (ΔH_m).

Cold crystallization of 2,6 PEKEKNK starts at 220 °C with an exotherm at 242 °C. Melting becomes detectable around 330°C. The melting temperature corresponding to the extremum of the melting endotherm is 380 °C. A shoulder is clearly present at 388 °C on the high temperature side of the melting endotherm. It probably results from the melting of a fraction of the sample which melted and recrystallized during

the scan. Alternatively it might result from an allotropic crystal form, since PAEKs display polymorphism when the ratio of ketone to ether groups reaches about two [23]. As will be illustrated below, this ambiguity can partly be resolved by performing X-ray scattering measurements under conditions similar to those of the DSC run. The cold crystallization and melting heats are –23.1 and 29.0 Jg^{-1} respectively, pointing to an initially almost fully amorphous sample [24]. The values of the thermal parameters for the commercial PEKEKK sample used here are similar to those obtained in the second DSC scan of the PEKEKK P1 sample by Rueda et al. [25] (T_g = 162.5 ºC, T_{cc} = 199.4 ºC, T_m = 372ºC and ΔH_m = 31.7$J\cdot g^{-1}$). The small differences suggest that the present sample has a somewhat lower molecular mass. The DSC scans for amorphous samples annealed at different temperatures for 30 min for PEKEKK and 1 hr for PEKEKNK are shown in Fig. 6 and the corresponding thermal properties are listed in Tab. 2.
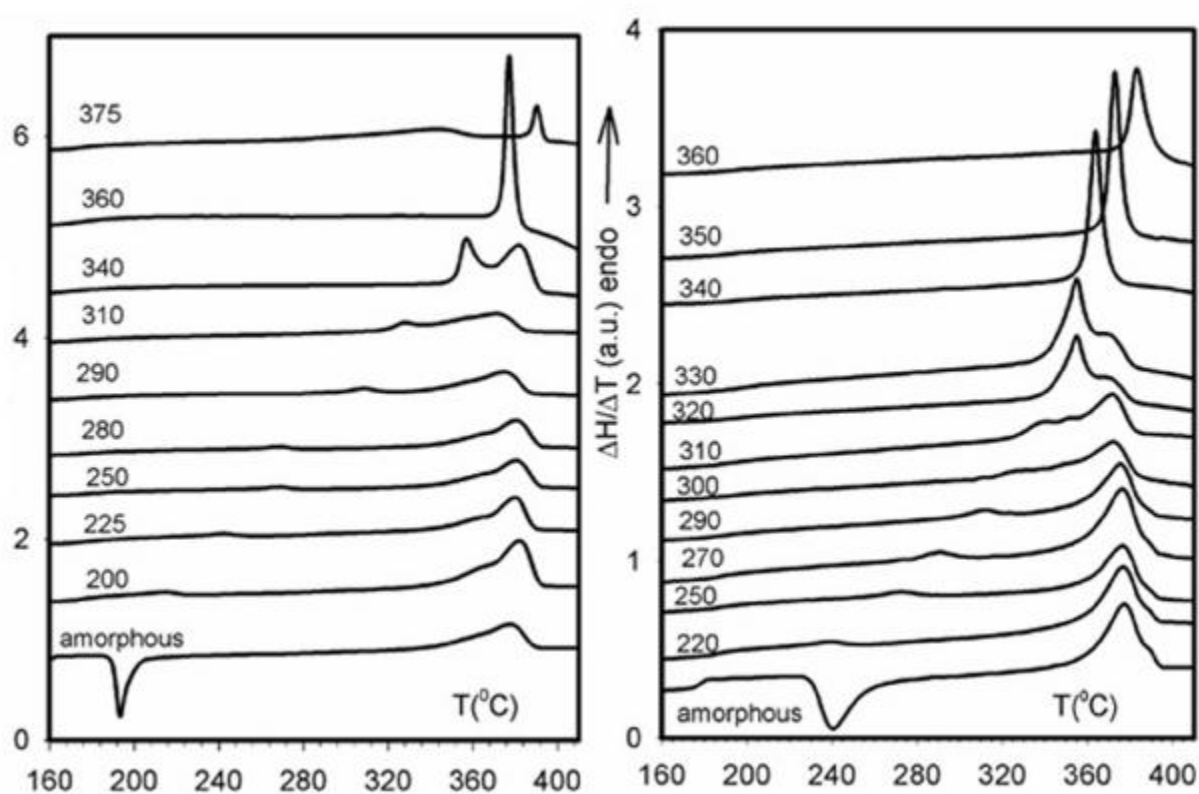
Fig. 6. DSC heating curves recorded at 10 °C/min for amorphous samples of PEKEKK annealed for 30 min at different temperatures (left) and amorphous samples of 2,6-PEKEKNK annealed for 1 hr (right) after heating at 10 °C/min.

Samples annealed at lower temperatures display two endotherms. The low temperature one sets in at a temperature close to the annealing temperature, progressively moves to higher temperatures and finally merges with the main melting endotherm. The PEKEKK sample annealed at 375 ºC has a broad maximum around 340 ºC, corresponding to the melting of material formed during cooling of the annealed sample or heating in the DSC scan, and a sharp melting peak at 390 ºC.

7

Tab. 2. Results of the DSC analysis for PEKEKK and 2,6-PEKEKNK.

PEKEKK

T_a (°C)	T_g (°C)	ΔC_p (J/gK)	T^{*1}_m (°C)	T^1_m (°C)	T^1_{end} (°C)	ΔH^1_m (J/g)	T^{*2} (°C)	T_{sh} (°C)	T^{*2}_{ons} (°C)	T^2_m (°C)	T^2_{end} (°C)	ΔH^2_m (J/g)	ΔH^{tot}_m (J/g)
200	175	0.22	203	215	225	2	270	363	362	382	400	73	75
225	174	0.24	230	242	260	3	270	362	361	380	400	49	52
250	174	0.23	256	269	290	3	300	363	359	381	400	43	46
280	176	0.15	285	294	320	3	322	366	368	386	400	43	46
290	178	0.18	296	308	320	4	325	361	349	375	395	35	39
310	178	0.20	315	328	337	-	-	358	-	371	395	-	52
340	168	0.25	351	357	368	-	300	-	362	382	401	-	78
360	172	0.40	-	-	-	-	350	-	374	377	385	-	48
375	175	0.29	-	-	-	-	280	-	387	390	400	-	45

2,6 PEKEKNK

T_a (°C)	T_g (°C)	ΔC_p (J/gK)	T^{*1}_m (°C)	T^1_m (°C)	T^1_{end} (°C)	ΔH^1_m (J/g)	T^{*2} (°C)	T_{sh} (°C)	T^{*2}_{ons} (°C)	T^2_m (°C)	T^2_{end} (°C)	ΔH^2_m (J/g)	ΔH^{tot}_m (J/g)
220	187	0.07	215	239	260	1	300	-	357	377	400	30	32
250	190	0.09	240	273	300	3	320	-	356	376	400	24	27
270	186	0.11	270	291	310	2	330	-	356	376	400	24	26
290	187	0.11	270	313	330	2	330	-	356	375	400	21	23
300	189	0.08	310	328	334	-	334	348	-	371	400	30	30
310	194	0.11	315	340s	-	-	-	351	-	372	400	-	28
320	190	0.08	320	348s	-	-	-	356	-	367	400	-	34
330	190	0.14	260	357	-	-	-	356	-	369	410	-	71
340	-	-	-	-	-	-	340	-	362	366	-	-	31
350	-	-	-	-	--	-	340	-	368	373	-	-	30
360	-	-	-	-	-	-	340	-	381	388	-	-	25

Starting from the amorphous state at room temperature, samples were heated at 10 °C/min and crystallized at different temperatures (T_a) for 30 min for PEKEKK and 1 hr for 2,6-PEKEKNK and cooled to room temperature at 10 °C/min. DSC traces were subsequently recorded during heating at 10 °C/min and the values of the temperature (T_g) and heat capacity change (ΔC_p) at the glass transition, start (T^{*1}_m), maximum (T^1_m), end (T^1_{end}) and enthalpy (ΔH^1_m) of the low temperature endotherm corresponding to the melting of crystals formed at T_a (for non-overlapping endotherms) were determined; Start of second range (T^{*2}), position of shoulder (T_{sh}), onset (T^{*2}_m), maximum (T^2_m), end of second range (T^2_{end}) and enthalpy (ΔH^2_m) corresponding to the main melting endotherm and total melting enthalpy (ΔH^{tot}_m). (s=shoulder).

Crystal Structure of PEKEKK and 2,6-PEKEKNK

The WAXD fiber patterns of stretched films of PEKEKK and 2,6-PEKEKNK (Fig. 7, Tab. 3) were indexed by analogy with that of PEEK [6,8].

For PEKEKK, the orthogonal cell dimensions are a = 0.776 nm, b = 0.602 nm and c = 0.993 nm for form I, and a = 0.414 nm, b = 1.119 nm and c = 0.993 nm for form II in agreement with previous values [23]. For 2,6 PEKEKNK the orthorhombic unit cell obtained by linear fitting is: a = 0.778(6) nm, b = 0.613(3) nm and c = 5.52(3) nm.

With four repeating units per unit cell, the calculated crystal density is 1.379 g.cm^{-3}. The length of the c-axis corresponds as expected to about five times the value found for the subcell in most PAEKs, which has typical dimensions of a = 0.78 nm, b = 0.59 nm, c = 0.99 nm [23]. Given that only the c-parameter differs from that of the PAEK's

family, the crystal structures of PEEK [6, 8] and PPO [5] with two macromolecular chains in an orthorhombic cell with Pbcn symmetry were used as the basis for modeling that of 2,6 PEKEKNK.
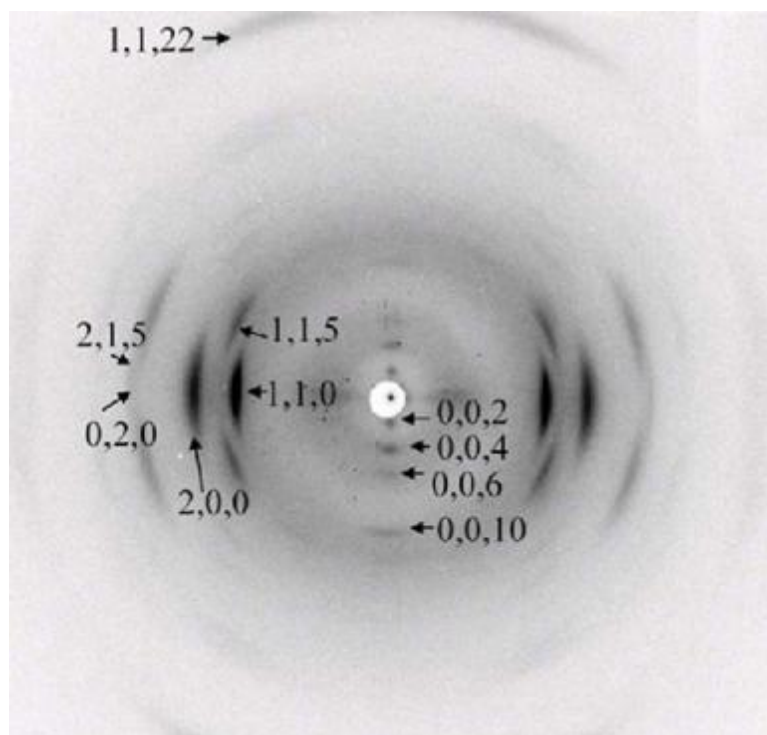

Fig. 7. Wide-angle X-ray diffraction pattern of a stretched sample of 2,6-PEKEKNK illustrating the indexation of the stronger reflections.

Tab. 3. X-ray data obtained from the WAXD pattern of a stretched 2,6 PEKEKNK sample. (h,k,l) Miller indices, observed (d_{obs} nm) and calculated (d_{calc} nm) spacings, observed (F_{obs}) and calculated (F_{calc}) structure factors.

| h	k	l	d_{obs}	d_{calc}	F_{obs}	F_{calc}	h	k	l	d_{obs}	d_{calc}	F_{obs}	F_{calc}
1	1	0	0.482	0.481	259	284	1	2	5	0.276	0.277	104	85
2	0	0	0.385	0.385	316	410	3	1	5	0.232	0.238	155	164
0	2	0	0.306	0.308	155	64	1	1	10	0.364	0.362	86	69
2	2	1	0.238	0.240	112	34	1	1	12	0.334	0.331	96	44
1	3	0	0.197	0.198	164	176	2	1	10	0.282	0.280	87	137
0	0	2	2.776	2.740	28	16	2	1	12	0.265	0.266	115	91
0	0	4	1.330	1.370	69	23	1	1	16	0.282	0.279	99	66
0	0	6	0.938	0.913	83	18	0	0	10	0.552	0.548	163	34
1	1	17	0.271	0.268	100	50	2	1	17	0.231	0.229	99	119
1	1	5	0.439	0.440	185	154	2	1	5	0.313	0.313	208	204
1	1	22	0.223	0.221	168	163	0	2	22	0.194	0.194	144	172
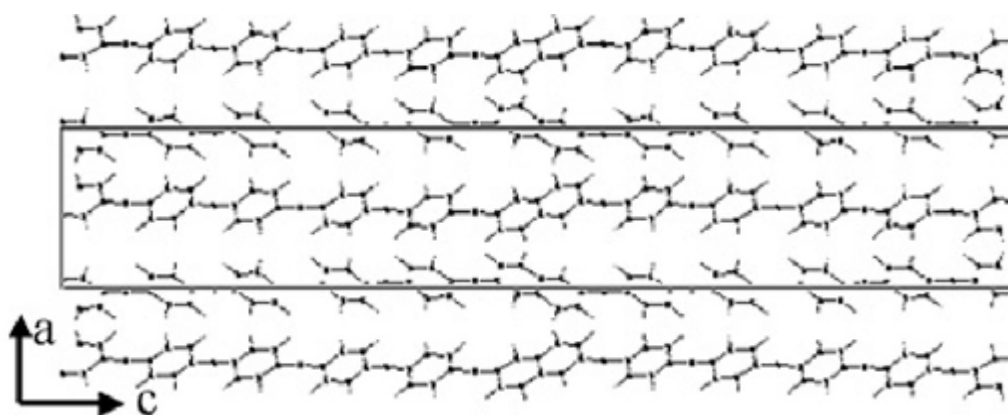
Fig. 8. View down the b-axis of a model of the crystal structure of 2,6-PEKEKNK based, by analogy with PEEK, on an orthorhombic cell with Pbcn symmetry. Note that ether and ketone links are parallel to the bc-plane.

Ketone and ether linkages can be interchanged without distortions of the chain and unit-cell [7-8, 23] and chains form zigzags consisting of two aryl units and ether or ketone linkages along the c-axis as in PPO, PEK, PEKK, PEEK and PEKEKK. The distance between these repeating units is about 1 nm.
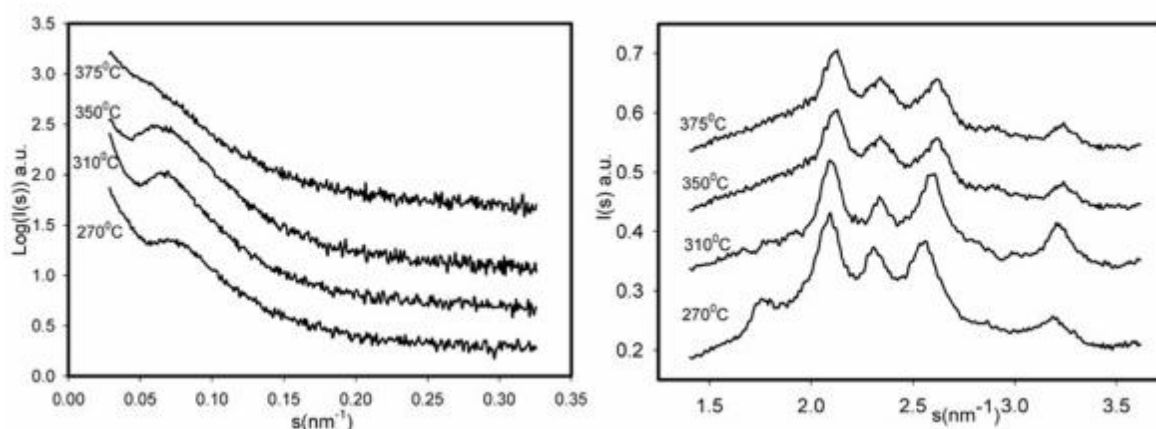

Fig. 9. Room temperature SAXS (left) and WAXD (right) patterns of PEKEKK samples annealed for 30 min at different temperatures as indicated. Note the characteristic 020 reflection of form II at s = 1.8 nm^{-1} in the WAXD pattern of the sample annealed at 270 ºC.The following set of internal coordinates (distances d and angles α) selected from previous structural studies [8,9,26-33] was used to compute the Cartesian coordinates of the atoms in the chain: aryl groups: d_{C-C} = 0.1395 nm, α = 120°, d_{C-H} = 0.1085 nm; ether links: d_{C-O} = 0.136 nm, α = 124°; ketone links: d_{C-C} = 0.147 nm, α = 126°, $d_{C=O}$ = 0.125 nm, $\alpha_{C-C=O}$ = 117°, torsional angles of aryl groups = 37°. The c-axis repeat distance (5.467 nm) in the resulting Pbcn unit cell (Fig. 8) is close to the experimental one (5.52 nm).

As pointed out by Wakelyn [7], if one considers the ketone and ether linkages to be distinct, the repeating unit along the c-direction in PEEK should consist of six aryl units. Similarly, as a result of the presence of naphthalene in the 2,6-PEKEKNK monomer the repeating unit consists of two monomers, with 8 phenyls, 2

10

naphthalenes, 6 ketone and 4 ether links. In addition to the perturbations due to interchange of ether and ketone links and the chain packing resulting from the relative position of these linkages in close packed chains [26], it is also necessary to consider the impact of the relative position of the naphthyl group.

The values of the observed structure factors taking into account Lorentz, polarization and multiplicity factors and those calculated with the crystallographic Powder Cell software [34] are given in Tab. 3. After scaling the observed and calculated intensities (squared structure factors) to the same average, the agreement in the overall pattern of weak and strong reflections yields a residual

$$R = \sum \left\| F_{obs} \right| - \left| F_{calc} \right\| / \sum \left| F_{obs} \right| = 0.3 \tag{1}$$

Although not entirely satisfactory, this seems reasonable given the approximations and justifies the analogy with PEEK. It also indicates that the packing in 2,6-PEKEKNK is also mainly governed by the overall extended chain conformation and orthorhombic symmetry. Comparison of the WAXD patterns of PEKEKK and 2,6-PEKEKNK in Fig. 9 and 10 also highlights the structural similarity between the two compounds. When PEKEKK and 2,6-PEKEKNK are crystallized in conditions similar to those used for DSC the two samples behave, however, quite differently. The PEKEKK samples display polymorphism, which is detectable in the WAXD pattern by the presence of the characteristic 020 reflection of form II [23], when crystallized from the amorphous state at temperatures below 300 ºC (Fig. 9, right) and transiently during some of the heating ramps to higher temperatures. This effect is, however, detected neither in the SAXS pattern nor in the DSC traces.
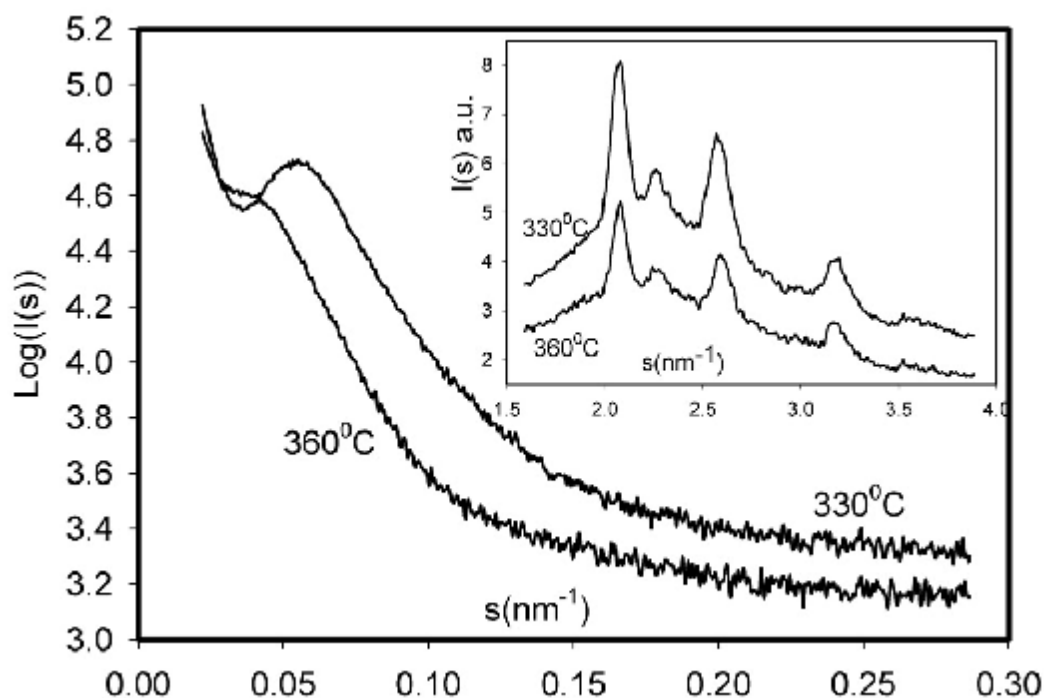

Fig. 10. Room temperature SAXS and WAXD (insert) patterns of 2,6 PEKEKNK samples after crystallization from the amorphous state and annealing for 1 hr at 330 and 360 °C.

For the two materials investigated here and in contrast with previous reports [35] for PEKEKK, no delay was observed in the appearance of traces of crystallinity in the SAXS and WAXD patterns. The long periods determined at room temperature from the maximum of $s^2I(s)$ increase with crystallization temperature from 12 nm at T_c = 220 ºC to 20.5 nm at 360 ºC for 2,6-PEKEKNK and from 11 nm at 180 ºC to 15 nm at 375 ºC for PEKEKK. No indication of polymorphism was found in the WAXD patterns of 2,6-PEKEKNK, neither during the heating scans nor after isothermal crystallization for 1 hr (Fig. 10).

Comparison of the DSC traces in Fig. 6 with the time courses of the integrated SAXS intensities ($s^2I(s)$) during melting of PEKEKK and 2,6-PEKEKNK samples obtained after annealing at different temperatures (in Fig.11) is of interest.
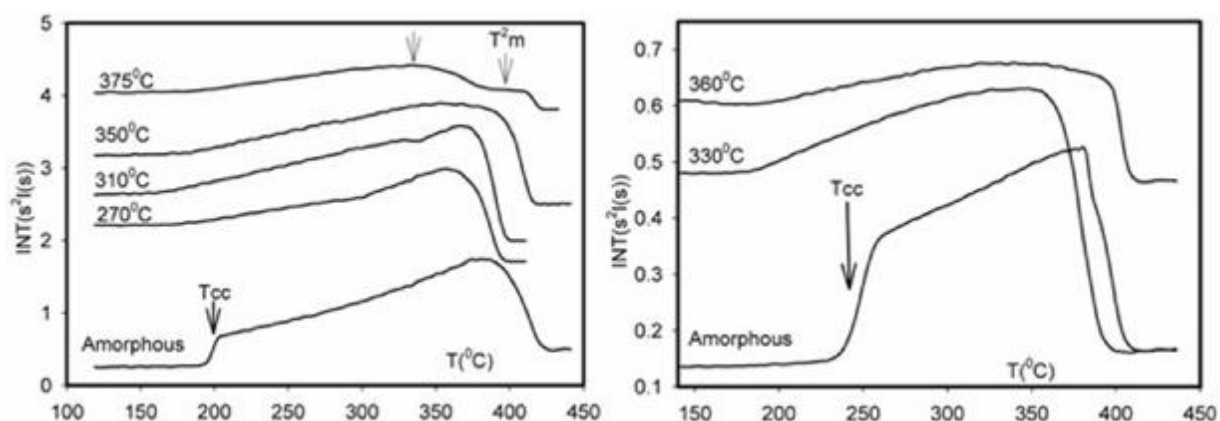

Fig. 11. Evolution of the integrated SAXS intensity for $0.02 \leq s \leq 0.2$ nm^{-1} during heating scans at 10 °C/min of an amorphous sample and samples annealed at different temperatures for PEKEKK (left) and PEKEKNK (right). Note the jump in intensity at the cold crystallization temperature (T_{cc}) of the amorphous sample. Note also the broad feature around 340 °C and melting at T^2_m = 390 °C for the PEKEKK sample annealed at 375 °C as also observed in the DSC traces in Fig. 6 (left). For the amorphous 2,6- PEKEKNK sample compare the shoulder around 388 °C with that in the DSC trace in Fig. 5.

The main features of the DSC traces - cold crystallization, double melting in the PEKEKK sample annealed at 375ºC and variation in final melting temperature - are also detected in SAXS. The integrated intensity of the sample annealed at 310 ºC decreases slightly around 340 ºC which corresponds to the end of the first endotherm. Similarly, the shoulder on the high temperature side of the melting endotherm of amorphous 2,6-PEKEKNK is clearly visible in the time course of the integrated SAXS intensity. The fact that the polymorphic transition in PEKEKK is only detected in the WAXD pattern [35] can be attributed to the fact that it occurs with a negligible volume (density) change. It does not have much influence on the SAXS intensity, which depends on the difference between the electron density of the crystalline and amorphous phase, nor on the enthalpy of the system.

The DSC and X-ray results obtained on the annealed samples are thus consistent with the melting/recrystallization of material formed during annealing and subsequent melting of all material at higher temperatures.

Conclusions

The crystalline structure and chain-packing of 2,6-PEKEKNK are very similar to that of the "pure" PAEKs and its thermal behavior parallels that of PEKEKK. The structural modification due to the naphthyl group in 2,6-PEKEKN results in a repeating unit with two monomers, in contrast with the unit cell of commercial PAEKs which contains two phenyl rings and two chemical links. In contrast with the situation for PEKEKK, no sign of polymorphism could be detected for 2,6-PEKEKNK. The presence of the naphtyl group increases the rigidity of the chain compared to other PAEKs. The glass transition temperature is 20 ºC but the melting temperature is only 2 ºC higher than for PEKEKK.

Experimental part

Materials

Triphosgene, phenyl ether, thionyl chloride and methanol (Sigma-Aldrich) were used as received. 1,2-Dichloroethane (Sigma-Aldrich) was distilled before use. High purity 2,6-naphthalene dicarboxylic acid was a generous gift from Dr. E. Paschke (Amoco). Its acid chloride derivative was obtained by boiling the acid in thionyl chloride followed by recrystallization of the crude acid chloride from the thionyl chloride-dichloroethane mixture. Anhydrous aluminum chloride (Sigma-Aldrich) was sublimed before use. 1,4-Bis-(4-phenoxy) benzophenone was prepared with a slight modification to the previously published procedure [13]: solid triphosgene [11] was added as a 0.15 M solution in 1,2 dichloroethane to a solution of phenyl ether in dichloroethane. The crude product was recrystallized twice from a toluene-ethanol mixture.

Poly(aryl ether ketone ether ketone ketone) or PEKEKK (Ultrapek®) was kindly supplied by BASF.

Viscosity

Viscosity was measured with a Ubbelohde viscometer taking the intrinsic viscosity as the mean of the reduced and inherent viscosities extrapolated to zero concentration. Measurements were made in methane sulfonic acid at 25 °C with solutions having initial concentration around 1gdl^{-1}. Five dilutions were used to cover a concentration range from 0.2 to 1 gdl^{-1}. The solutions did not present any polyelectrolyte behavior.

Density

The density of the solid samples was determined by flotation with an accuracy of 10^{-4} gcm^{-3} and that of the solutions with a Mettler-Toledo MA-300 densimeter using mixtures of n-heptane and carbon tetrachloride as done previously for PEEK [15].

Differential Scanning Calorimetry (DSC)

DSC experiments were performed at a heating rate of 10 °C/min in a DSC 2920 calorimeter (TA Instruments) under nitrogen using about 5 mg sample. The curves were analyzed using the TA Universal Analysis software to obtain the glass (T_g), the cold crystallization (T_c) and the melting temperatures (T_m), the increase in heat capacity at the glass transition (ΔC_p) and the heats of melting (ΔH_m) and

crystallization, (ΔH_c). Temperatures and heats of transition are precise to 0.1 °C and 0.1 Jg^{-1}, respectively.

NMR

The NMR spectra were collected on a Bruker AMX-300 spectrometer operating at 300.14 MHz for the ^1H spectra and 75.47 MHz for the ^{13}C spectra. A 5% (m/v) solution of 2,6-PEKEKNK in a 1:1 (v/v) $CDCl_3/CF_3COOH$ mixture was used for all measurements.

X-ray Diffraction

Wide angle X-ray diffraction patterns (WAXD) of oriented samples were recorded on imaging plates using a Kiessig camera with pinhole collimation and Ni-filtered Cu Kα radiation delivered by a Rigaku RU200 rotating anode. The imaging plates were scanned on a FujiX BAS-3000 analyzer with a resolution of $(50 \, \mu m)^2$. They were processed using the "X-Ray" software [16] which (i) finds the center of the image, (ii) integrates small angular sectors of the reflections and (iii) indexes first the equatorial and meridional reflections and subsequently the azimuthal ones.

Small angle X-ray scattering (SAXS) and WAXD patterns were collected simultaneously in 20s frames using two linear gas position sensitive detectors with delay line readout [17] on the X33 camera of the EMBL [18] at the DORIS III storage ring of the Deutsches Elektronen Synchrotron (DESY) in Hamburg. The samples were wrapped in thin aluminum foils and subjected to the same thermal programs as in the DSC measurements in a Linkam heating stage. The SAXS and WAXD data were collected in the ranges $0.1310^{-2} \leq s \leq 0.33 \, nm^{-1}$ and $1.1 \leq s \leq 3.8 \, nm^{-1}$, respectively (s = 2sin$\vartheta/\lambda$, where 2$\vartheta$ is the scattering angle and λ = 0.15 nm the wavelength of the incident X-rays) and evaluated using standard procedures [19].

Acknowledgements

References

[1] Cotter, R. J. *Engineering Plastics. A Handbook of Polyarylethers.* Gordon and Breach Publishers: Basel, **1995**.
[2] Kricheldorf, H. R. In *Handbook of Polymer Synthesis, Part A*; Kricheldorf, H. R., Ed.; Marcel Dekker: New York, **1992**; p 545.
[3] Lakshmana Rao, V. J. *Macromol. Sc., Rev. Macromol. Chem. Phys. C*, **1995**, *35*, 661-712.
[4] Dawson, P. C.; Blundell, D.J. *Polymer* **1980**, *21*, 577.
[5] Boon, J.;Magré, E. P. *Makromol. Chem.* **1969**, *126*, 130.
[6] Rueda, D. R.;Ania, F.;Richardson; A.;Ward, I. M.;Balta-Calleja, F. J. *Polymer Comm.* **1983**, *24*, 258.
[7)] Wakelyn, N. T. *Polymer Comm.* **1984**, *25*, 306.
[8)] Fratini, A. V.;Cross, E. M.; Whitaker, R. B.;Adams, W. W. *Polymer* **1986**, *27*, 861

[9] Petraccone, V.;Pirozzi, B.;Corradini, P.;Giunchi, G. *Polymer* **1991**, *2*, 396.

[10] Blundell, D. J.;Liggat, J. J.;Flory, A. *Polymer* **1992**, *33*, 2475.

[11] Gardner, K. H.;Hsiao, B. S.;Matheson Jr, R. M.;Wood, B. A. *Polymer* **1992**, *33*, 2483.

[12] Zolotukhin, M. G.;Gileva, N. G.;Sedova, E. A. *Dokl. Akad. Nauk. SSSR* **1989**, *304*, 378.

[13] Zolotukhin, M. G.;Dosière, M.;Fougnies, C.;Villers, D.;Gileva, N. G.;Fatykhov, A. A. *Polymer* **1995**, *36*, 3575.

[14] Eckert, H.; Forster, B. *Angew. Chem.* **1987**, *99*, 922.

[15] Kaito, A.;Nakayama, K. *J. Polym. Sci., Polym. Phys. Ed.* **1994**, *32*, 691.

[16] Dammer, C.; Leleux, P.; Villers, D.; Dosière, M. *Nucl. Instr. and Meth.* **1997**; B132:214.

[17] Rapp, G.; Gabriel, A.; Dosière M.; Koch, M. H. J. *Nucl. Instrum. Methods* **1995**, A357,178.

[18] Koch, M. H. J.; Bordas, J. *Nucl. Instrum. Methods* **1983**,208,461.

[19] Fougnies, C.;Damman, P.;Villers, D.;Dosière M.; Koch, M. H. J. *Macromolecules* **1997**, 30, 1385.

[20] Zolotukhin, M. G.;Rueda, D. R.;Balta Calleja, F. J.;Cagiao, M. E.;Bruix, M.; Sedova, E. A. ; Gileva, N. G. *Polymer* **1997**, *38*, 1471.

[21] Daoust, D;Godard, P.;Devaux, J.;Legras, R.;Strazielle,C. *Polymer* **1994**, *35*, 5498.

[22] Zolotukhin, M.G., Rueda, D.R., Balta Calleja, F.J., Cagiao, M.E., Bruix, M. Bulai, A., Gileva, N.G., Van der Elst, L. *Polymer* **1997**, 38, 3441.

[23] Blundell, D. J.;Newton, A. B. *Polymer* **1991**, *32*, 308.

[24] Holdsworth, P. J.;Turner-Jones, A. *Polymer* **1971**, *12*, 195.

[25] Rueda, D.R.;Zolothukin, M.G.;Cagiao, M.E.;Balta Calleja, F.J.;Villers, D.; Dosière, M. *Macromolecules* **1996**, 29, 7016.

[26] Chen, C. L.;Chang, J. L.;Su, A. C. *Macromolecules* **1992**, *25*, 1941.

[27] Hay, J. N.; Kemmish, D. J. *Polym. Commun.* **1989**, *30*, 77-80.

[28] Abraham R. J.;Haworth, I. S. *Polymer* **1991**, *32*, 121.

[29] Zimmermann, H. J.; Könnecke, K. *Polymer* **1991**, *32*, 3162.

[30] Verot, S.; Battesti, P. *Can J. Chem.* **1995**, *73*, 581.

[31] Colquhoun, H. M.; O'Mahony, C. A.; Williams, D. J. *Polymer* **1993**, *34*, 218.

[32] Cebe, P. *J. Matls. Sci.* **1988**, 23, 3721.

[33] Bassett, D. C.;Olley, R. H.;Al Raheil, I. A. M. *Polymer* **1988**, 29, 1745.

[34] Kraus, W.;Nolze, G. *J. Appl. Cryst.* **1996**, 29, 301.

[35] Rueda, D.R.,Garcia Gutierrez, M.C., Ania, F., Zolotukhin, M.G., Balta Calleja, F.J. *Macromolecules* **1998**, 31, 8201.